Multifactor Aging of HV Generator Stator Insulation Including Mechanical Vibrations

M. B. Srinivas, T. S. Ramu
Department of HV Engineering,
Indian Institute of Science, Bangalore, India.

ABSTRACT

The longtime behavior of solid electrical insulation is influenced by the nature as well as the magnitude of applied stresses. Much work has been done over the years to model and understand insulation degradation under single and combined electric and thermal stresses. However, efforts aimed at including mechanical stress as an additional interactive aging term in the existing models appear to be scanty. In the present work, the authors describe experimental methods for acquisition and analysis of insulation failure data when fatigue stresses, due to vibration, are present with electric and thermal stresses. An empirical model, based essentially on an Eyring relation, together with a fatigue crack propagation approach (in line with Miner's cumulative damage model) has been presented. Attempts have been made to verify this model experimentally.

1. INTRODUCTION

THE long time behavior, or aging, of electrical insulation has been a topic of intensive study for quite some time. It has been established that the rate of aging, or the rate at which the essential properties of an insulation reduce, is not only a function of the magnitude but also of the nature of applied stress. During the past twenty years or so, it has been increasingly felt that the amount of aging in apparatus insulation is sensitive also to the way in which the stresses occur, *i.e.* whether singly or in combination.

The most important types of stresses to which the insulation is subjected are electrical, thermal and mechanical. Considering the conductor insulation in a HV rotating machine, this insulating structure encounters the three stresses at the same point in time.

In order to understand the processes leading to insulation degradation, it is necessary to develop a physical model which connects the nature and magnitude of the various stresses and the time at which a failure ensues. One of the simpler methods of building the model is to assume that the stresses are applied in sequence and arrive at the distribution pattern of times to failure of nominally identical specimens. This type of testing is called the sequential testing and was applied to insulation failure degradation acquisition some time ago. This model is defective in the sense that the existence is ignored of interaction of failure modes due to the simultaneity of application of stresses, which gives rise to secondary degradation processes of significant magnitudes.

In an earlier work, problems associated with combined electrical and thermal aging of insulation structures have been studied in detail [1]. Several other attempts have been made in trying to work out a formalism, at least on an empirical basis, for describing the aging failure mechanism due to combined stress [2–4]. Some of these formalisms have given sufficiently accurate information on the aging processes involved and permit an approximate evaluation of insulation life.

In a recent work [5], a contribution to understanding aging of overhang insulation of HV machine stator conductors by mechanical stress, in vibration, has been highlighted. In that paper, a tangible multifactor degradation model including vibration of the overhang was proposed.

Kelen [6] covers the details of multifactor functional

0018–9367 $3.00

testing on HV machine bars. This work is directed towards establishing a credible test method to account for the rapid degradation of epoxy-mica insulation systems under mechanical and electrical stresses.

The present work describes experimental methods for acquisition and analysis of insulation failure data when fatigue stresses due to vibration are also present with electrical and thermal stresses. An empirical model, based essentially on an Eyring relation together with a fatigue crack propagation approach (in line with Miner's cumulative damage model [7]) has been presented. Attempts have been made to verify this model experimentally. A comparison has been provided of the estimated lives based on proven statistical techniques and the experimentally obtained insulation life.

2. THEORETICAL

SEVERAL aspects of insulation aging under combined electrical and thermal stresses have been covered earlier [1–3]. The model for failure of insulation in the presence of mechanical stresses can be shown to be an inverse power law, similar to the electrical failure model.

The conductor overhang is viewed as a freely vibrating cantilever beam, where the maximum stress occurs at the fixed point. The failure caused by vibration is due to fatigue damage, because when the extremity of overhang is pushed up by a force F such that the central line of the conductor is displaced by an amount δ, layers of insulation on the opposite faces of the conductor in the direction of applied force are subjected to tensile and compressive stresses, respectively. A sinusoidal variation of the force on insulation layers induces alternate tensile and compressive stresses and therefore constitutes a fatigue.

Structural engineers [8] have proposed a phenomenological failure model for a cantilever beam which includes a crack type defect, however small. This defect gets enlarged with repeated application of a force. The rate of extension of the crack with N stress reversals is empirically

$$\frac{dx}{dN} = C\sigma^m x^q \tag{1}$$

in which σ is the strain, x is the crack length, C, m and q are constants. σ is given by the ratio of stress S to Young's modulus Y

$$\sigma = \frac{S}{Y} \tag{2}$$

Therefore, Equation (1) becomes

$$\frac{dx}{dN} = C'S^m x^q \tag{3}$$

Integration of (3) gives

$$\frac{x^{-q+1}}{-q+1} = C'S^m N + \tau \tag{4}$$

where τ is a constant of integration.

Now, let the initial crack length be x_0 so that

$$\frac{x_0^{-q+1}}{-q+1} = \tau \tag{5}$$

Suppose we define a condition at which the crack length x acquires a critical value x_c, then the ratio (x_c/x_0) can be treated as a critical quantity and the structure is deemed to have failed no matter how this value has been reached.

defining $\gamma' = x_c/x_0$, Equation (4) can be simplified to

$$NS^m = \text{constant} \tag{6}$$

Now

$$N = f_m t \tag{7}$$

where f is the mechanical frequency of vibration and t is the time duration. Since f_m is constant, Equation (6) becomes

$$tS^m = K_m \tag{8}$$

where K_m is a constant.

This Equation is formally similar to the inverse power law for electrical aging.

As mentioned earlier, the overhang can be thought of as a freely vibrating cantilever beam with maximum stress occurring at the fixed point. Since the beam has its mass distributed, modes of vibration other than the fundamental could also be present, depending upon the clamping, the length, and the mass of the overhang. Figure 1 shows a vibrating beam and its first four natural frequencies and Table 1, lists corresponding magnitudes. In view of the possibility of existence of other modes, it is necessary to consider stress levels associated with each one. However, when the fundamental mode has the dominating effect, other modes of vibration could be neglected.

Now, the equation of motion of a freely vibrating cantilever beam firmly fixed at one end can be written as

$$\rho s\frac{\partial^2 z}{\partial t^2} + \frac{\partial^2}{\partial x^2}\left[YI\frac{\partial^2 z}{\partial x^2}\right] = 0 \tag{9}$$

where z is the instantaneous amplitude which is a function of displacement x and time t, that is $z = f(x,t)$. Therefore, Equation (9) becomes

$$\rho s\frac{\partial^2 f(x,t)}{\partial t^2} + \frac{\partial^2}{\partial x^2}\left[YI\frac{\partial^2 f(x,t)}{\partial x^2}\right] = 0 \tag{10}$$

where I is the area moment of inertia, ρ the density of the vibrating structure, and s is the cross section area.

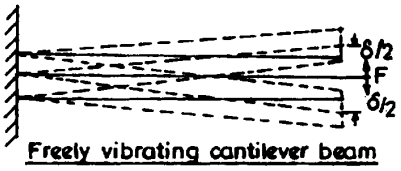

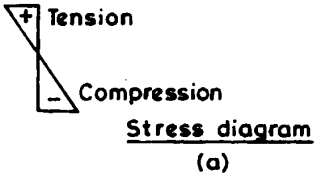

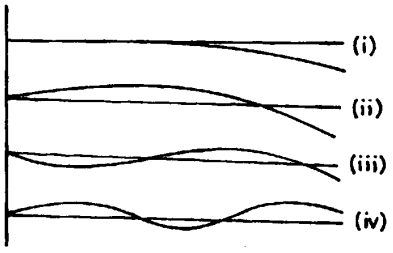

No.	λ	f
i	3·52	120 Hz
ii	22·4	240Hz
iii	61·7	360Hz
iv	121·0	480Hz

Figure 1.

Vibration patterns of a freely oscillating cantilever beam with its first four natural frequencies.

The natural frequencies of such a vibrating system can be arrived at by solving the above equation under relevant boundary conditions given in [8]

$$f_n = \frac{\lambda}{2\pi}\sqrt{\frac{YI}{\rho s l^4}} \tag{11}$$

in which l is the length of the free overhang and λ the coefficients tabulated in [8].

2.1 CALCULATION OF MECHANICAL STRESS

The mechanical stress S is the maximum plane stress in the overhang and this occurs at the fixed point. If deflection δ of the free overhang is produced by a force F, then it can be shown that

$$\delta = \frac{Fl^3}{6YI} \tag{12}$$

Usually, the value of δ is known and I is a function of the geometry of the system. Using this formula, the force F can be calculated for any δ which in turn can be used to calculate the fatigue stress as shown in Table 1.

2.2 MULTISTRESS MODEL

The insulation life at any electric stress E and at room temperature can be expressed by the empirical power law

$$L = KE^{-n} \tag{13}$$

in which K and n are constants.

When the insulation is under thermal stress, the life at any temperature T is given by the Arrhenius relation

$$L = A\exp\frac{B}{T} \tag{14}$$

where A is a constant and B is related to the activation energy ΔG_E of the aging process given by $B = \Delta G_E/k$, k being the Boltzmann's constant.

When the insulation is subjected to a mechanical stress S, the life can be expressed by power law as proved earlier, and is given by

$$L = K_m S^{-m} \tag{15}$$

where K_m and m are constants.

In an earlier work [1], the life under combined electric and thermal stresses was treated as following the power law assuming the power law constants as temperature dependent

$$L(T,E) = K(T)E^{-n(T)} \tag{16}$$

This expression is weighted by an Arrhenius term to take into account the non-zero thermal aging

$$L(T,E) = K(T)E^{-n(T)}\exp\frac{B}{T} \tag{17}$$

When mechanical stress is also present in addition to thermal and electrical stress, the power law constants can be treated as functions of T and S and the above expression should be weighted, in addition, by a mechanical aging term

$$L(E,T,S) = K(T,S)E^{-n(T,S)}\exp\frac{B}{T}S^{-m} \tag{18}$$

Now, if E_0, T_0, S_0 are the operating stresses, then

$$L_0 = L(E_0,T_0,S_0)K(T_0,S_0)E^{-n(T_0,S_0)}\exp\frac{B}{T_0}S_0^{-m} \tag{19}$$

By virtue of the phenomenological fact that the endurance coefficient is a decreasing function of other supplementary

stresses T and S, and assuming, as a first approximation, that the interaction between these stresses is small, it is possible to express $n(T,S)$ as a linear combination of the endurance coefficients when the thermal and mechanical stresses are present separately with electric stress

$$n(T,S) = n(T) + n(S) \tag{20}$$

Also, it is known phenomenologically that $n(T)$ and $n(S)$ are decreasing functions of T and S respectively

$$\begin{aligned} n(S) &= a - bS \\ n(T) &= c - \frac{d}{T} \end{aligned} \tag{21}$$

When S is very small or zero and T is less than or equal to the room temperature, then $n(T,S)$ is given by

$$n(T,S) = a + c = n \tag{22}$$

Therefore, life L can be written as

$$L = L_0 K(T,S) \left[\frac{E^s}{E_0^s}\right]^b \left[\frac{E}{E_0}\right]^{-n} \left[\frac{E^{1/T}}{E_0^{1/T}}\right] \left[\frac{S}{S_0}\right]^{-m} \times \exp\left[\frac{\Delta G E}{K}\left(\frac{1}{T} - \frac{1}{T_0}\right)\right] \tag{23}$$

To determine the constants in the above Equation, experiments have to be conducted at single electric, thermal and mechanical stresses, combined electrical and thermal stresses and combined electrical, thermal and mechanical stresses.

3. EXPERIMENTAL

In running the aging experiments, different designs of test specimens and experimental designs have been adopted. The more important considerations in drawing up an experimental schedule are the duration of experimentation, cost of running aging experiments and the stress acceleration factors. A detailed commentary on these aspects can be found in [1, 11]. Full size coils of 11 kV rotating machine stator conductor bars insulated with epoxy-bonded mica, as shown in Figure 2, have been used in all experiments involving mechanical stresses. The edges of the conductors were rounded off longitudinally to relieve the stress concentration. The coils were divided into about 15 sections by wrapping aluminum foil around the conductor insulation with sufficient gap (typically 20 to 30 mm) between the sections. In this way, a sample size of about 15 per coil could be achieved.

During aging experiments where mechanical stresses were absent, short length of coil sections 13 to 18 cm long cut from nominally identical conductor bars mentioned above were used. In this case, the sample size is typically between 10 and 12.

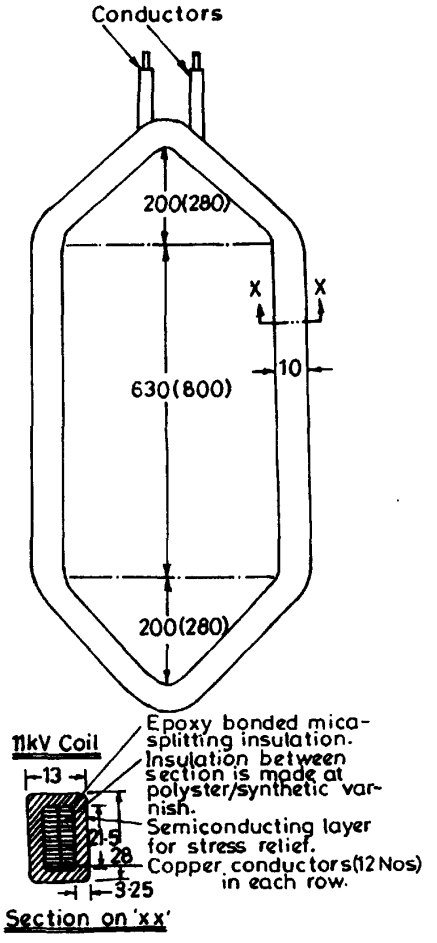

Figure 2. Coil geometry.

Experiments were conducted both under single and multifactor stress conditions. Table 2 shows the various stresses and stress combinations employed during the aging experiments. Figure 3 shows the complete test assembly used for conducting vibration experiments. The hexagon shaped conductor was laid flat on a steel fixing frame securely grouted to ground. The conductor was fixed on to the frame as shown in the Figure by coil fixing pads. The overhang portion of the conductor rests firmly on the moving element of the vibration generator (exciter). In vibration tests, it is essential to ensure that the exciter produces a truly sinusoidal vibration force and that this force is imparted effectively to the vibrating member.

To characterize the vibration, several parameters are to be considered; the more important among them are the frequency, the displacement, and the acceleration. The

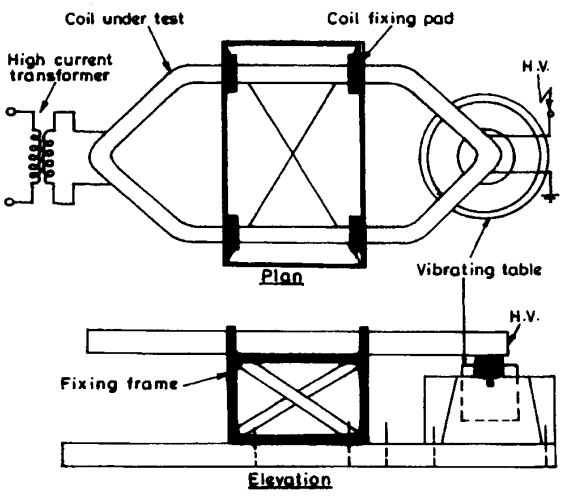

Figure 3.
Schematic diagram of vibration test facility.

Table 1.
Details of mechanical stress aging experiments.

Displacement (μm)	Stress (N/cm^2)	Modes of Vibration* n	f_n
1200	66.4	1	120
		2	764
1000	55.4	3	2102
800	44.2	4	4130

*n = order of harmonic

f_n = natural frequency of order n

acceleration G produced by the exciter is given by

$$G = \frac{F}{m_p + m_e} \tag{24}$$

where m_p is the mass of the test specimen (pay load) and m_e is the mass of the moving element.

In vibration testing, it is not possible to fix all the vibration parameters at the same time. Therefore, one should fix at least two parameters and vary the others. In the series of experiments conducted, the frequency and the acceleration have been fixed. This permits variation of the amplitude over a considerable range. It was possible to achieve accelerations of 10 g at 120 Hz when the displacement was between 100 and 1200 μm (peak to peak).

Table 2.
Magnitude of stresses and stress combinations.

Type of Stress	Single Stress			Combined Stress	
Stress Applied	E	T	M	E+T	E+T+M
E (kV)	20	-	-	20	20
	22			22	22
	24			24	24
	26			26	26
				+	+
T (°C)	-	155	-	180	180
		180		210	210
		210		230	230
					+
M (N/cm^2)	-	-	44.2	-	44.2
			55.2		55.2
			66.4		66.4

E - Electrical
T - Thermal
M - Mechanical

The high-current transformer used for heating the coil shown in Figure 3 was provided with HV isolation between primary and secondary and the vibration exciter was electrically isolated from the coil.

4. RESULTS AND ANALYSIS

In the foregoing analysis, unless otherwise mentioned, failure is defined as a 50% reduction in the breakdown strength. The method used to arrive at this value consists in drawing a small proportion of the total number of specimens (2 to 3) at each inspection time slot and performing a dielectric strength test on them with continuously increasing voltage. It is possible that the dielectric strength (E_d) obtained this way not be equal to the 50% E_d. As the aging test proceeds, this procedure is repeated over different time windows until the desired level of reduction in E_d is achieved. It is important to note that the time required to reach 50% E_d is so inordinately long, even when the accelerating factors are higher, that it would not be possible to continue experiments over such durations of time. In the present work, a type-I censored experimental plan in which the experiments were terminated after a lapse of between 2000 and 3000 h to save time and cost, has been used. A method of determination of time to 50% E_d, based on an empirical formula, can be found in [12].

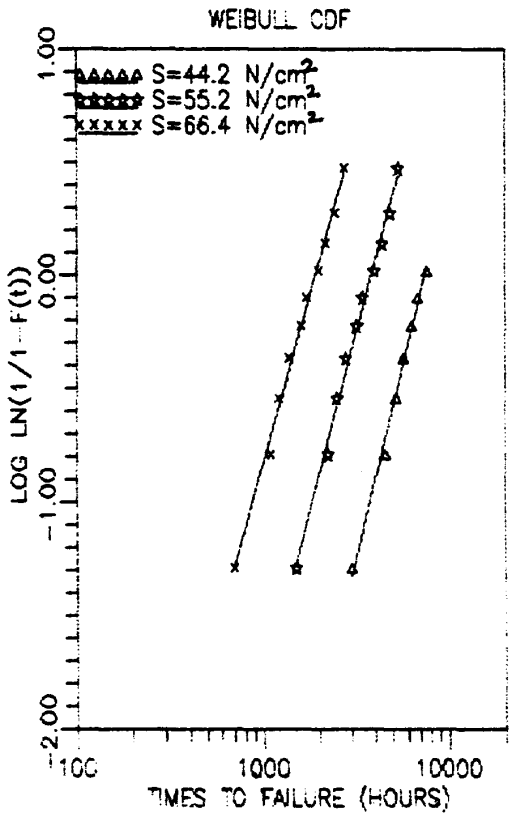

Figure 4.
Weibull plots of mechanical stress failure data.

The times to failure of overhang insulation under vibration (fatigue) stresses are assumed to follow a two-parameter Weibull distribution since the degradation is a weak link process. During this study, the coil was also subjected to electric stress and hence the failure is due to the combined stress effect. Figure 4 shows a Weibull cumulative probability plot of the data. In Figure 5, the inverse power law plot for the above data is shown from which the endurance coefficient n and constant K can be evaluated. Figures 6 to 8 depict the Weibull plots under combined electrical and thermal stresses of epoxy-mica insulation failure data while in Figures 9 to 12, similar plots when mechanical stress is also present have been included. For the sake of brevity, data at two temperatures namely, 180 and 230°C have been presented. The inverse power law plots of these data are presented in Figures 13 to 15. In order to study the dynamics of aging, the changes in the power law parameters and Weibull shape parameter with different stress combinations were investigated and Figures 16 and 17 describe the systematic changes of these parameters. The different stresses, their combinations and their mechanical characterization

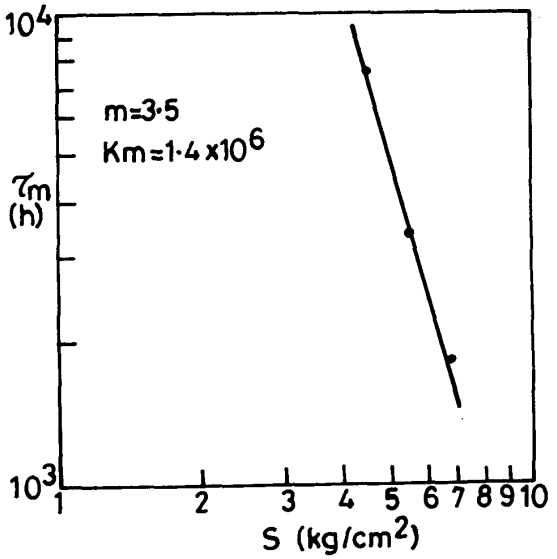

Figure 5.
IPM plot for single mechanical stress failure data.

Table 3.
Estimated values of power law parameters under combined electrical, thermal and mechanical stresses.

S (N/cm²)		0			55.2			66.4		
T (°C)		Low	Est	Up	Low	Est	Up	Low	Est	Up
155	n	7.9	8.4	8.9		-			-	
	K	4×10^{14}								
180	n	6.7	7.3	7.9	5.6	6.6	7.6	5.1	6.3	7.6
	K	4.9×10^{12}			2.4×10^{11}			7.4×10^{10}		
210	n	6.1	6.9	7.7	5.0	6.1	7.2	4.6	5.8	7.0
	K	6.1×10^{11}			3.3×10^{10}			8.8×10^{9}		
230	n	5.5	6.5	7.5	4.7	5.8	6.9	4.3	5.5	6.7
	K	6.0×10^{10}			4.6×10^{9}			1.5×10^{9}		

Low - Lower Confidence Bound
Est - Estimated Value
Up - Upper Confidence Bound

of aging are included in Tables 1 and 2. Tables 3 and 4 cover the results of aging study including the life estimates using the suggested model. Table 5 compares the life times estimated using the model with experimentally obtained life times. A sample calculation for estimating the multifactor-stress life is shown in Appendix 1.

To highlight the experimental data acquisition, graph-

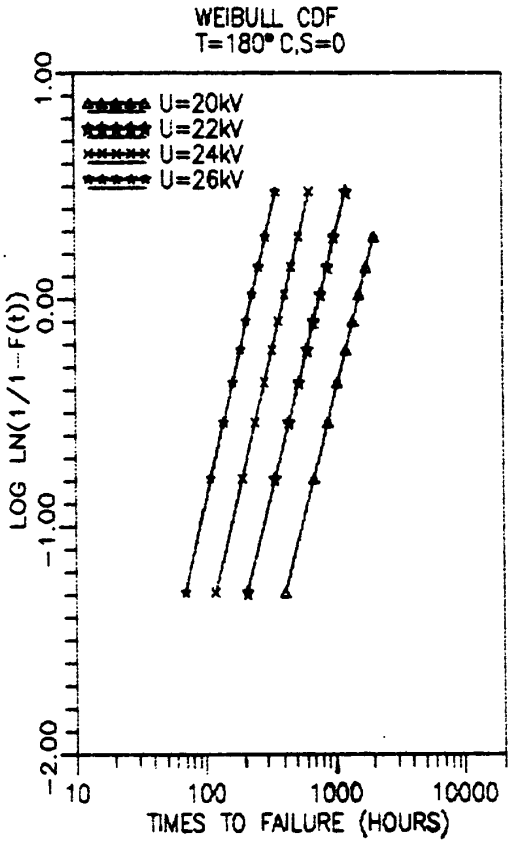

Figure 6.

Weibull plots of combined electric and thermal stress failure data.

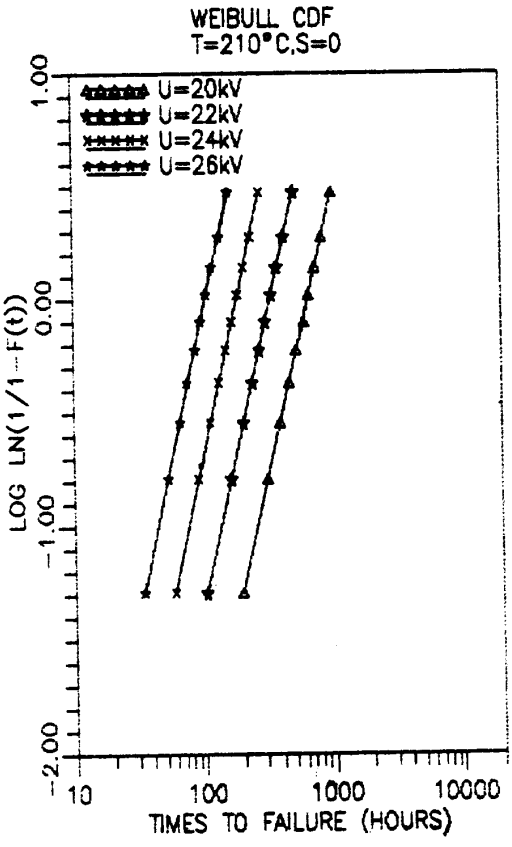

Figure 7.

Weibull plots of combined electric and thermal stress failure data.

Table 4.

Estimated values of shape and scale parameters of Weibull distribution at different stresses.

		S = 0			S = 55.2 N/cm^2			S = 66.4 N/cm^2		
$T_{(\delta C)}$	U (kV)	22	24	26	22	24	26	22	24	26
155	β	2.03	2.17	2.25	-	-	-	-	-	-
	τ	2117	1019	520	-	-	-	-	-	-
180	β	2.28	2.40	5.20	2.39	2.42	2.45	2.42	2.47	2.58
	τ	777	411	230	331	187	110	258	150	90
210	β	2.56	2.61	2.64	2.61	2.70	2.75	2.62	2.68	2.75
	τ	333	183	105	214	127	77	144	87	55
230	β	2.73	2.80	2.85	2.88	2.92	3.04	3.19	3.38	3.62
	τ	113	64	45	75	45	29	62	38	25

ical methods have been used. However, in the calculation of point and interval estimates of the power law parameters and insulation life, a proven statistical technique in maximum likelihood has been applied. The stress employed in the series of experiments were such that there was a need, in some cases, for terminating the experiments before all the specimens have failed, thus generating a censored data set. A modified maximum likelihood technique has been used in analyzing such data [9].

5. DISCUSSION

BASED on preliminary tests, experiments and consultation with generating station engineers, the peak to peak amplitude of normal vibrations of the overhang was fixed at 100 μm. In order to obtain failure data in a reasonably short time, an accelerating factor of 12, giving a maximum peak to peak amplitude of 1200 μm has been used. To obtain the parameters of inverse power law model under mechanical stress, fewer specimens (4 to 6) were used to minimize the cost of running aging experiments.

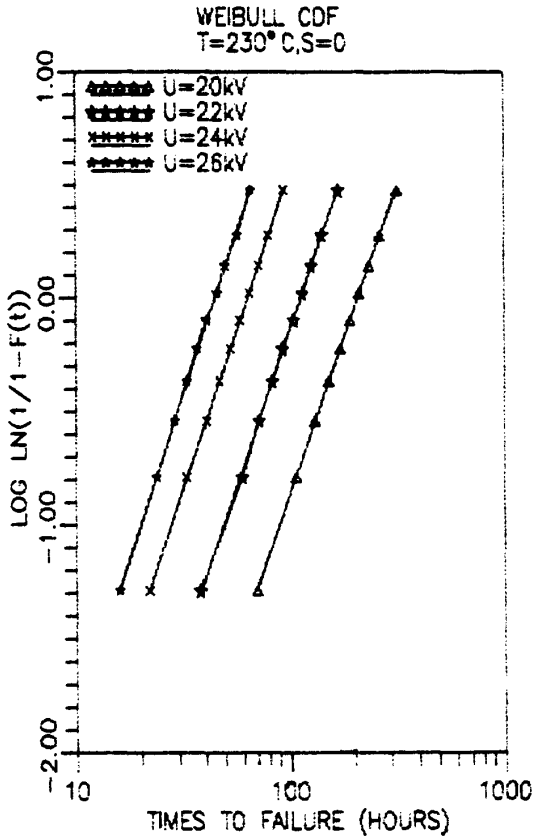

Figure 8.

Weibull plots of combined electric and thermal stress failure data.

The times to failure under fatigue loading (vibration), are assumed to follow an extreme value probability distribution similar to that under electrical aging process. In the case of epoxy-bonded mica insulation, which is a two component system, damage may occur due to deflaking of mica laminate or debonding of mica from the epoxy. A second possibility of damage exists in the opening of straight cracks through the body of the insulation. When electric stress is also present in addition to mechanical stress, the first possibility results in the insulation becoming weaker due to increased partial discharge activity in the fissures and the crevices, leading to failure. In the second case, the crack in the direction of the force also happens to be in the direction of the electric field and hence progressive breakdown due to treeing would occur. Normally both the possibilities exist.

The methods of modeling multifactor failure of insulation are very unclear to date. Different researchers [1–3] have proposed phenomenological models by considering

Table 5.
Comparison of experimental and estimated lives.

Ageing Stresses			L_{Est} (h)	L_{Expt} (h)
U (kV)	T (^{o}C)	M (N/cm^2)		
20	180	0	1556	1400
24	180	55.4	186	190
20	210	0	643	680
26	210	55.4	77	80
20	230	0	290	200
26	230	66.4	24	25

L_{Est} - Estimated Life (See Equation (23)
L_{Expt} - Experimental Life

(Extracted from corresponding Weibull plots)

only two types of stresses. The modeling usually begins with the approach suggested by Eyring, applied with modifications by Zoellener and Endicott [10]. A combined electrical and thermal aging model of Simoni [2] has also been derived based on the Eyring formalism. A modified version of this was presented by Ramu [1]. In this version, the inverse power law parameters n and K were assumed to be temperature dependent and a correction factor was incorporated to take into account the variation in the parameters with applied stress. The correction was effected by altering the forms of the power law constants so as to reflect the phenomenological results.

A formalism for degradation of insulation when more than two stresses are present at the same time does not appear to have been attempted earlier. In this direction, efforts were made in the authors' laboratory to try to work out expressly an equation for probable life of electrical insulation when the simultaneous electrical, thermal and mechanical stresses are applied. In effect, the approach followed is similar to an earlier one in that the basic expression for life was still assumed to be an inverse power law with the understanding that the parameters of the power law are functions of temperature and mechanical stress.

In obtaining the parameter estimates of the suggested model, the changes in the power law parameters $K(T, S)$ and $n(T, S)$ have been arrived at using Equations (21) to

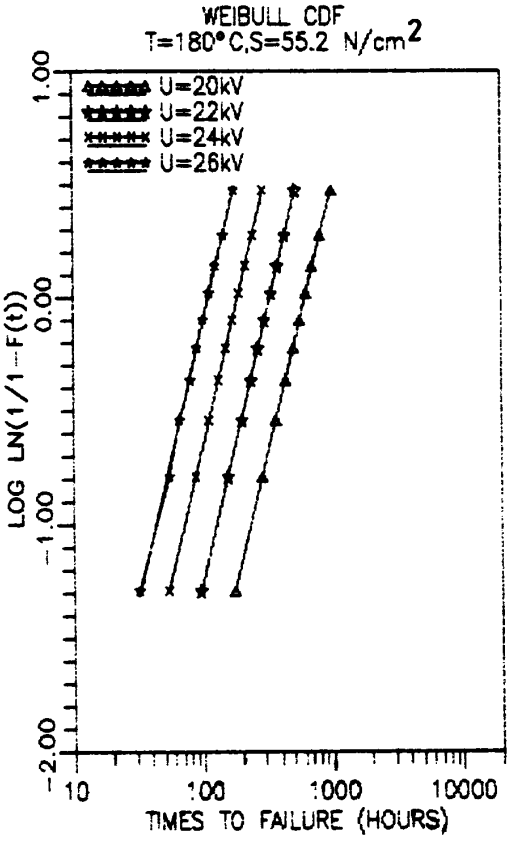

Figure 9.

Weibull plots of combined electric and thermal stress failure data.

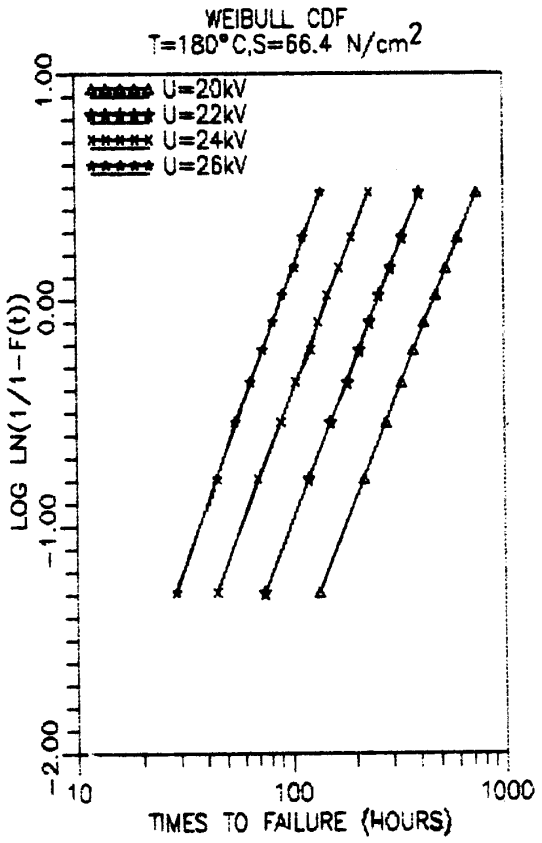

Figure 10.

Weibull plots of combined electric and thermal stress failure data.

(23) and by conducting an aging study involving thermal and electrical stress and electrical, thermal and mechanical stresses. The application of the model in studying the insulation life can be made by conducting the single as well as combined stress aging experiments to work out the correction factors required due to the simultaneous presence of the other stresses. When these parameters are known, the life equation can be used at any other stress level as in the case of single stress life estimation.

To understand the mechanism on a statistical basis, the changes in the estimates of under different aging stress conditions have been incorporated in Figure 17. The information derivable from this characteristic is that when the accelerating factors are small, a weak link aging process (shown by straight lines on a Weibull paper) in which β is invariant with respect to stress takes place. As opposed to this, the other two characteristics show a curvature indicating that β is not invariant with stress. This implies that at high stresses, after a certain duration of time, the instantaneous mortality becomes so high that all times to failure will occur within a reasonably short duration of time. This is reflected in Figures 18 and 19 where the hazard function increases steeply at higher stresses, thus indicating impending failure. It is known from the statistical theory of failure that when $\beta > 3.0$, the distribution of times to failure becomes almost normal. In fact, such a situation arises when electric, thermal and mechanical stresses of magnitudes $\gtrsim$ 24 kV, 210°C and $\gtrsim$ 44 N/cm^2 respectively, are applied. A similar qualitative analysis can be made of the physical inverse power law model assumed in this work. Figure 16 gives an idea of the changes in K and n at different stresses. More information on these parameters is presented in Tables 3 and 4.

An important observation regarding the Weibull plots (Figures 6 to 12), is that they are very linear. One may wonder as to how this linearity is preserved even when several failure mechanisms are at work. This point is

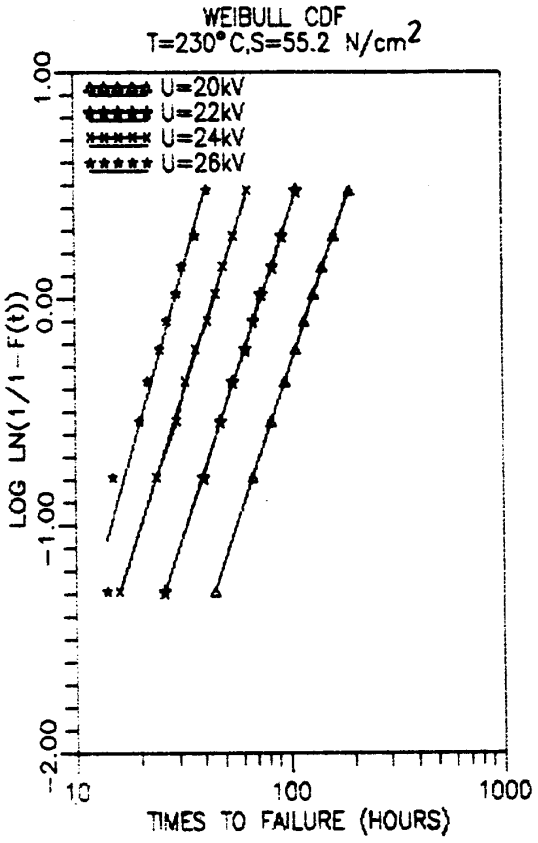

Figure 11.

Weibull plots of combined electric and thermal stress failure data.

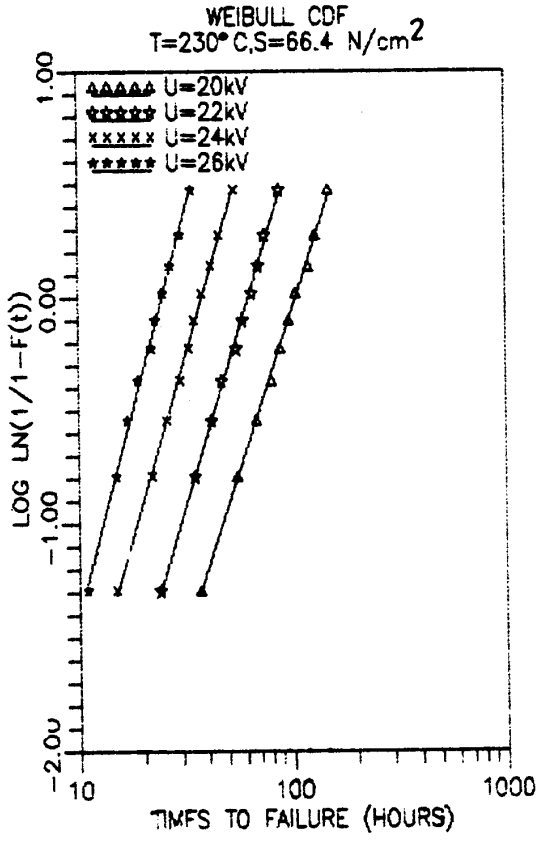

Figure 12.

Weibull plots of combined electric and thermal stress failure data.

clarified in the following.

The multifactor failure model has been built expressly on the assumption that the electrical stress is the main degenerating factor in view of the fact that it follows an inverse power law. Further, the mechanical degradation due to vibrations (or fatigue) also obeys an inverse power law. The aging process in the presence of these two stresses can be visualized in terms of a weak-link mechanism when the stresses are applied either individually or combined and hence the posterior distribution of life times is still Weibull.

Considering now the effect of thermal stress, the degradation mechanism is due to a physico-chemical reaction rate process and follows the classical Arrhenius relation. The statistical distribution of times to failure is found to follow a log-normal type distribution in two parameters. The joint distribution of failure times when all the stresses are present, could however represent a departure from the extreme behavior. The fact that the Weibull plots are perfectly linear indicates that the thermal degrada-

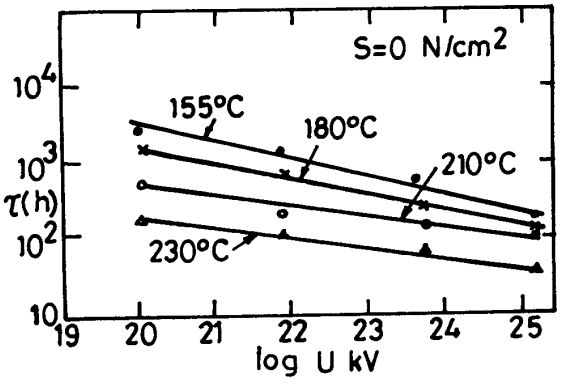

Figure 13.

Power law plots of combined electric and thermal stress failure data at different temperatures.

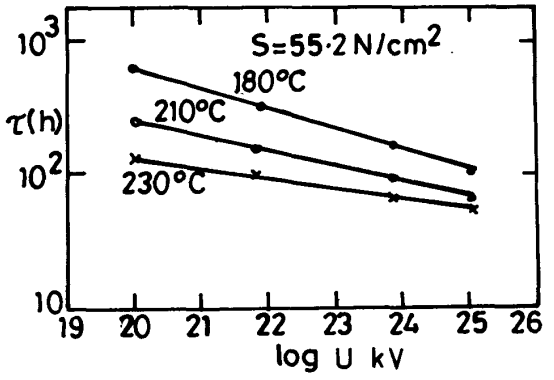

Figure 14.
IPM plots for different temperatures at $S = 55.2$ N/cm^2.

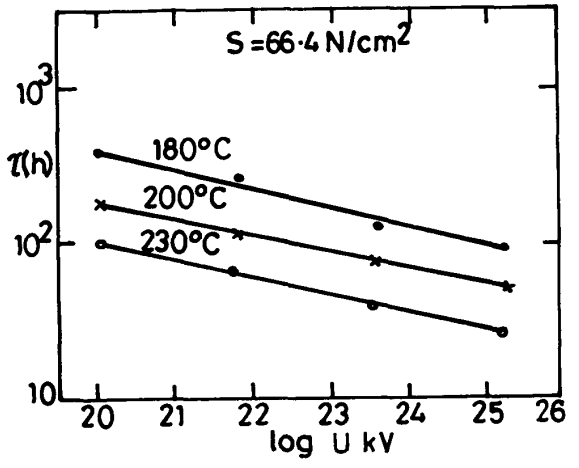

Figure 15.
IPM plots for different temperatures at $S = 66.4$ N/cm^2.

tion process is acting only as a secondary aging process in promoting aging as mentioned earlier and is not involved directly in causing a complete failure. This means that the effect of thermal aging can be brought into the model by multiplying the abstract degradation term by a factor which is a function of temperature and when normalized, works out to a factor less than unity. This assumption has now been vindicated by the experimental results. However, as may be seen from Figure 17, the value of the shape parameter as a function of stress increases rapidly beyond a certain level of stress acceleration, indicating that the shape parameter is not invariant with respect to stress. This suggests that very different processes of failure, which cannot be combined into a single process, could be in force when the experiments are conducted at extremely high stress levels.

In designing an experimental plan, care has been taken

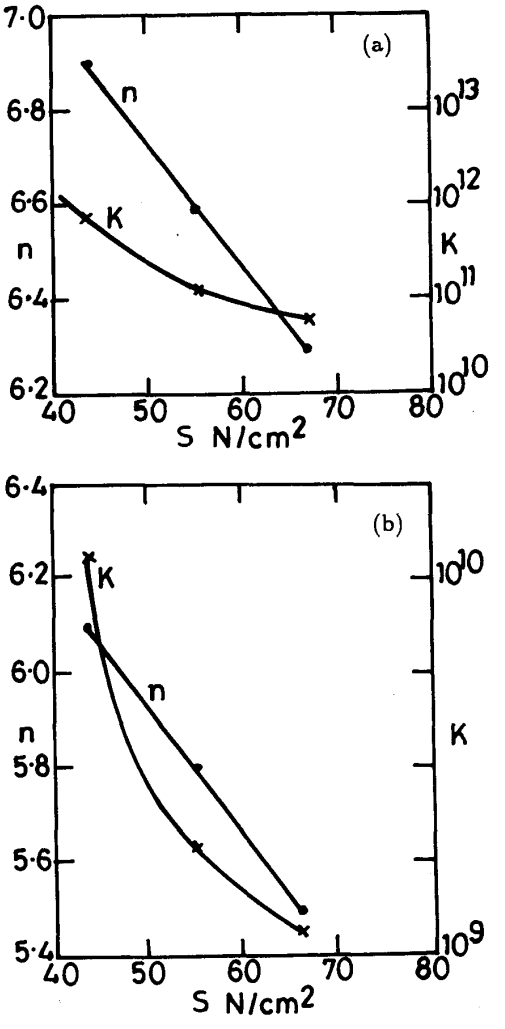

Figure 16.
Variation in $K(S)$ and $n(S)$ as a function of mechanical stress at (a) 180°C, (b) 230°C.

to choose the accelerating factors in such a way as not to violate the condition that the Weibull shape parameter be invariant with respect to stress. This is therefore the reason that the Weibull characteristics are sensibly linear.

6. CONCLUSIONS

THE work reported in this paper provides a means of estimating life of HV machine insulation under multifactor stress including mechanical vibration. The assumption that the electric stress is the main cause of failure and the mechanical and thermal stresses only promote the degradation indirectly is vindicated by the experimental results. The information concerning the variability of β with respect to electric stress beyond a certain limit can

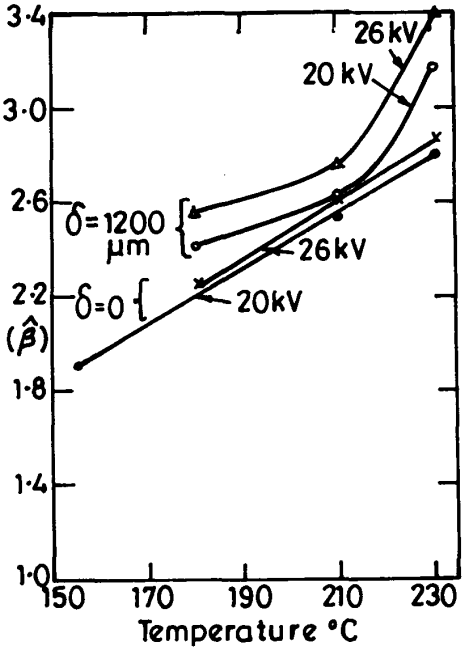

Figure 17.

A plot of the shape parameter β *vs.* temperature at different electric and mechanical stresses.

be used as a qualitative measure of the degree of aging under multifactor stress.

7. APPENDIX

7.1 A SAMPLE CALCULATION FOR ESTIMATING THE MULTIFACTOR STRESS LIFE

Equation 23 can be rewritten with slight modifications as

$$\ln L = \ln L_0 - n \ln \frac{E}{E_0} - m \ln \frac{S}{S_0} + \frac{B}{\theta} + bS \ln \frac{E}{E_0} + \frac{d}{\ln(E/E_0)} \tag{25}$$

In this Equation, A and B are constants of the Arrhenius model, K and n are constants of inverse power law model for electric stress, K_m and m are constants of inverse power law model for mechanical stress, and b and d are constants of multifactor life model.

The values of these parameters at 155°C (operating temperature for class-F insulation) are

$$\begin{array}{lll} A = 4.54\times10^{-1} & B = 4.00\times10^{3} & K = 6\times10^{11} \\ n = 1.4\times10^{6} & K_m = 1.4\times10^{6} & m = 3.51 \\ b = 0.05 & d = 2.07\times10^{3} & \end{array} \tag{26}$$

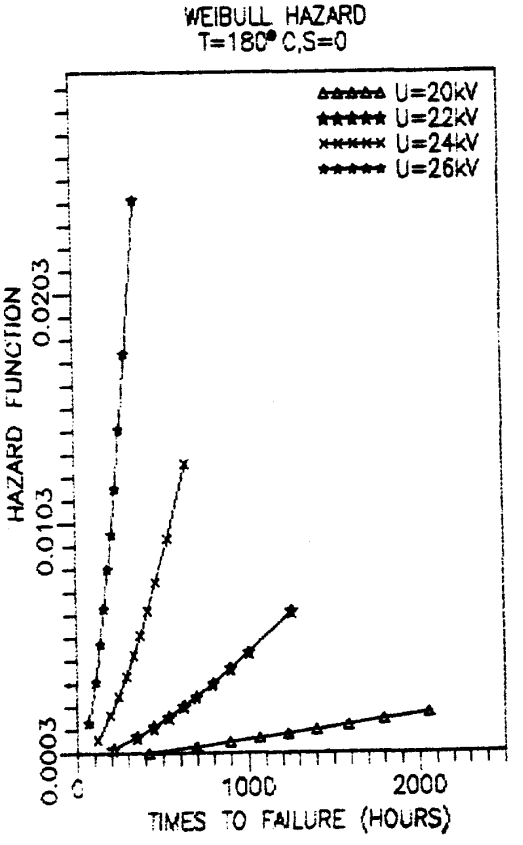

Figure 18.

Hazard plots for combined electrical and thermal stress failure data.

The other parameters entering into the calculation are L_0, the electrical life = 25 years at the normal operating voltage $U_0(11/\sqrt{3}$ kV). T_0, the normal operating temperature = 155°C= 428 K. S_0, normal operating mechanical stress = 0.55 N/cm^2 (ascertained from generating station engineers).

The stresses at which the life is estimated are

$$\begin{aligned} U &= 20\text{kV} \\ S &= 66.2\text{N/cm} \\ T &= 230 \leftrightarrow C \ = 503K \end{aligned} \tag{27}$$

Substituting these values in the life equation, life at above mentioned stresses can be estimated to be 376 h. The corresponding life from experiment is $\sim$ 240 h.

REFERENCES

[1] T. S. Ramu, "On the Estimation of Life of Power Apparatus Insulation under Combined Electrical and Thermal Stresses", IEEE Trans. Electrical Insulation, Vol. 20, pp. 70–78, 1985.

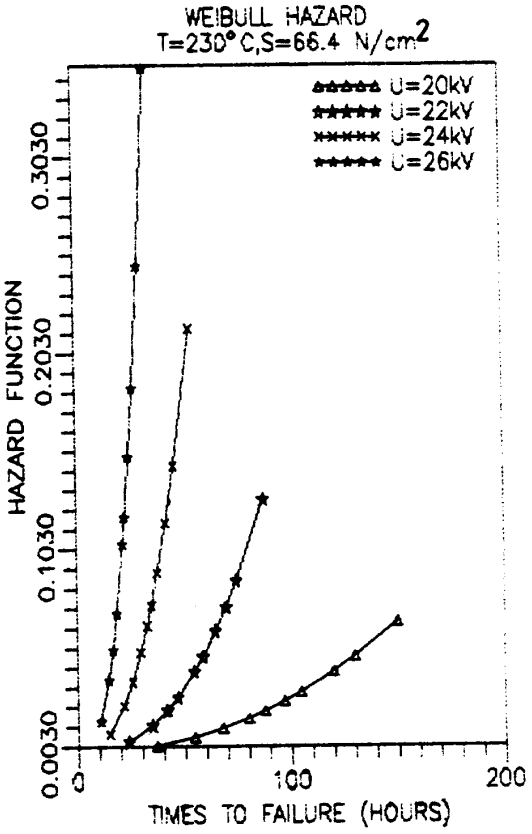

Figure 19.

Hazard plots for combined electrical, thermal and mechanical stress failure data.

[2] L. Simoni, "Life Models for Insulating Materials under Combined Thermal-electric Stress", Colloquim of Professional committee of IEE, Group-52, pp. 1–10, Dec. 1980.

[3] B. Fallou, C. Burgiere, "First Approach on Multiple Stress Accelerated Life Testing of Electrical Insulation", Annual report, CEIDP, NCR conf. Pocono, October 1979.

[4] P. Cygan, J. R. Laghari, "Models for Insulation Aging under Electrical and Thermal Multistress", IEEE Trans. Electrical Insulation, Vol. 25, pp. 923–934, 1990.

[5] T. S. Ramu, "Degradation of HV Generator Insulation under Mechanical, Electrical and Thermal Stresses", IEEE International Symposium on Electrical Insulation, Toronto, Canada, June 1990.

[6] A. Kelen, "Functional Testing of HV Generator Stator Insulation", Paper 15–03, Vol. 1, CIGRE, 1976.

[7] M. A. Miner, "Cumulative Damage in Fatigue", Journal of Applied Mechanics, pp. A159–A163, Sept. 1945.

[8] J. T. Broch, *Mechanical vibrations and shock measurements*, 4th edition, Bruel & Kjaer, Denmark, 1984.

[9] M. B. Srinivas, T. S. Ramu, "Monte Carlo Approach to Aging Data Acquisition and Analysis of Apparatus Insulation", Proc. CIGRE symp. on New and improved materials for Electro-technology, Vienna, Austria, May 1987.

[10] H. S. Endicott, J. A. Zoellener, "A Preliminary Investigation of the Steady and Progressive Stress Testing of Mica Capacitors", Proc. Fourth National symp. on Reliability and Quality control, IRE, pp. 6–8, NY, Jan. 1968.

[11] H. N. Geetha, M. B. Srinivas, T. S. Ramu, "Pulse-count Distribution as a Possible Diagnostic Tool for Assessing the Level of Degradation of Rotating Machine Insulation", IEEE Trans. Elec. Insul., Vol. 25, pp. 747–756, Aug. 1990.

[12] H. N. Geetha, T. S. Ramu, "Estimation of Residual Life in Electrical Insulation", IEE Conf. Dielectric Materials, Measurements and Applications (DMMA), Canterbury UK, June 27–30, 1988.

Manuscript was received on 3 January 1991, in revised form 13 April 1992.